Article

Not peer-reviewed version

Eco-Friendly Silver Nanoparticles Synthesized from Soybean By-Product with Nematicidal Efficacy against *Pratylenchus brachyurus*

Letícia Santana de Oliveira , Leila Lourenço Furtado , Francisco de Assis dos Santos Diniz , Bruno Leonardo Mendes , Thalisson Rosa de Araújo , Luciano Paulino Silva , Thaís Ribeiro Santiago *

Posted Date: 8 November 2023

doi: 10.20944/preprints202311.0514.v1

Keywords: green synthesis; soybean leaf extract; nematotoxic efficacy; plant-parasitic nematodes; migratory endoparasitic nematode; nanotechnology

Article

Eco-Friendly Silver Nanoparticles Synthesized from Soybean By-Product with Nematicidal Efficacy against *Pratylenchus brachyurus*

Letícia Santana de Oliveira [1], Leila Lourenço Furtado [1], Francisco de Assis dos Santos Diniz [1], Bruno Leonardo Mendes [1], Thalisson Rosa de Araújo [1], Luciano Paulino Silva [2] and Thaís Ribeiro Santiago [1,*]

[1] Departamento de Fitopatologia, Universidade de Brasília, 70910-900, Brasília, DF, Brazil; leticiasanoli2@gmail.com; leilafurtado24@hotmail.com; francisco.santos.diniz1996@gmail.com; bleomendes@gmail.com; thalissonaraujo76@gmail.com

[2] Laboratório de Nanobiotecnologia (LNANO), Embrapa Recursos Genéticos e Biotecnologia, PBI, 70770-917, Brasília, DF, Brazil; luciano.paulino@embrapa.br

* Correspondence: thais.santiago@unb.br

Abstract: This study explores an eco-friendly approach to synthesizing silver nanoparticles (AgNPs) using soybean leaf extracts, employing a reaction with silver nitrate at 65°C for 2.5 h. Optimal results were achieved at extract concentrations of 3.12 and 6.25 mg leaf mL^{-1}, termed 3.12AgNP and 6.25AgNP, respectively. UV-Vis spectrophotometric analysis between 350-550 nm exhibited a peak at 410-430 nm, along with a color transition in the suspensions from pale yellow to brown, indicating successful synthesis. Dynamic light scattering (DLS) further delineated favorable properties of these AgNPs, including nanometric dimensions (73–104 nm), negative charge, and moderate polydispersity, portraying stable and reproducible synthesis reactions. The bioreduction mechanism, possibly expedited by leaf extract constituents such as amino acids, phenolic acids, and polysaccharides, remains to be fully elucidated. Notably, the study underscored the potent nematicidal effectiveness of the biosynthesized AgNPs, especially 6.25AgNP, against *Pratylenchus brachyurus*, a common plant parasitic nematode in tropical soybean cultivation regions. *In vitro* tests illustrated significant nematicidal activity at concentrations above 25 µmol L^{-1}, while *in vivo* experiments displayed pronounced nematode population diminishment in plant roots, particularly with a 6.25AgNP rhizosphere application at concentrations of 500 µmol L^{-1} or twice at 250 µmol L^{-1}, attaining a reproduction factor below 1 without any morphological nematode alterations. The research highlights the potential of 6.25AgNPs derived from soybean leaf extracts in forging sustainable nematicidal solutions, marking a significant stride towards eco-friendly phytonematode management in soybean cultivation. This novel methodology signals a promising avenue in harnessing botanical resources for nematode control, propelling a greener agricultural horizon.

Keywords: green synthesis; soybean leaf extract; nematotoxic efficacy; plant-parasitic nematodes; migratory endoparasitic nematode; nanotechnology

1. Introduction

The battle against pest and pathogens is paramount for ensuring global food security, especially for staple crops such as soybean (*Glycine max*). Root lesion nematodes, particularly *Pratylenchus brachyurus* (Godfrey) Filip Schurr-Steekh, pose formidable challenges in this struggle, known for their devastating impact as documented by [1] and [2]. These phytonematodes pose a substantial threat to soybean cultivation, causing relevant yield losses due to their wide distribution, extensive host range, and the severe, often irreversible damage [3–5].

The presence of *P. brachyurus* is characterized by the emergence of dark, reddish-brown to black lesions on plant roots. Over time, these lesions coalesce, forming extensive necrotic areas resulting from the oxidation of root tissues. Additionally, as these nematodes penetrate and feed on plant roots, they can establish peculiar interactions with other phytopathogenic microorganisms, ultimately compromising plant health [6–8]. These nematodes thrive in tropical climates, taking advantage of

 doi:10.20944/preprints202311.0514.v1

favorable conditions and the abundance of host crops [9]. Their effectiveness is further amplified by their array of enzymes, which enable them to move through root tissues and subdue the plant's defenses [10–12].

While a myriad of management strategies has been deployed against *P. brachyurus*, many have fallen short in terms of long-term sustainability and efficacy [13–15]. With traditional methods waning, the scientific community is turning to innovative solutions. Among these, silver nanoparticles (AgNPs), particularly those green-synthesized from plant extracts, have emerged as potential game-changers. The prowess of AgNPs derived from various plant extracts in mitigating nematode threats is well-documented, pointing to their promise as potent nematicides.

AgNPs produced through green synthesis methods, particularly using plant leaf extracts, have attracted significant attention due to their effective management of plant-parasitic nematodes [16]. A plethora of recent research has underscored the efficacy of such AgNPs in controlling *Meloidogyne* species, through processes such as inhibition of egg hatching, obstructing entry of J2 juveniles into roots, and disrupting juvenile development [17–19]. Moreover, a study by [20] demonstrated the decline of *Heterodera sacchari* population and the concurrent enhancement of vegetative growth and yield in rice plants, resulting from the application of green-synthesized AgNPs.

The choice of reducing agents in the synthesis of nanoparticles is crucial in determining the physicochemical characteristics and toxic effects of AgNPs. Leaf extracts of plants, which contain compounds like amino acids, flavonoids, phenolic compounds, sugars, and terpenoids, not only reduce silver ions and stabilize the AgNPs but also regulate their growth, aggregation, and can enhance their nematotoxic activity [21–24]. For example, AgNPs synthesized using medicinal plant leaf extracts such as *Conyza dioscoridis*, *Melia azedarach*, and *Moringa oleifera* have demonstrated high efficacy against egg hatching and the J2 stage of *M. incognita* [25]. However, secondary metabolites in *C. dioscoridis* leaf notably enhanced the nematicidal effect of AgNPs compared with other treatments. Leaf extracts from a variety of plants, such as *Euphorbia tirucalli*, *Azadirachta indica*, *Curcuma longa*, *Acalypha wilkesiana*, *Senna siamea*, and *Ficus sycomorus*, have been successfully utilized in the biosynthesis of AgNP, demonstrating effectiveness in reducing phytonematode populations [26–30]. Interestingly, soybean, the very crop threatened by the nematodes, might hold the key to an effective countermeasure. Extracts from soybean leaves, an often-overlooked by-product, have shown promise for synthesizing potent AgNPs [31,32]. Nevertheless, the potential of these nanoparticles in combating plant parasitic nematodes has yet to be fully explored in research.

Our study delves into this uncharted territory, focusing on *P. brachyurus*, a nematode that does not form specialized feeding cells, thus representing a unique challenge. We venture to harness the potential of green-synthesized AgNPs from soybean derivatives, envisaging a sustainable and cyclical agricultural management approach. Our overarching goal is to amplify the value of soybean by-products in pest management, offering an innovative, sustainable, and efficient solution.

Given the unexplored potential of AgNPs synthesized from soybean components in controlling phytonematodes, our study sets out to undertake a comprehensive analysis, aiming to: (i) assess the effectiveness of AgNPs synthesized through green methods using various concentrations of soybean leaf extract; (ii) perform physical and chemical characterization of the synthesized nanoparticles; (iii) evaluate the *in vitro* and *in vivo* nematicidal activity of these AgNPs; (iv) investigate the biomolecules responsible for the reduction of Ag^{+} to Ag^{0} and the stabilization of the synthesized AgNPs; and (iv) study the mode of action of AgNPs on *P. brachyurus* specimens.

2. Materials and Methods

2.1. Soybean leaf extract

Healthy soybean plants (cv. Willians) were cultivated in a greenhouse at 25 ± 5°C at the University of Brasília, Brasília, Federal District, Brazil, for 45 days. The leaves were carefully harvested, washed thoroughly with a 1000× diluted neutral detergent solution, and rinsed with distilled water to remove any residue. The plant material was then air-dried at room temperature and stored in a sealed plastic bag at -20°C.

 doi:10.20944/preprints202311.0514.v1

To prepare the plant extract, 2 g of the cold leaves were cut and mixed with 20 mL of boiling distilled water for 2 min. The extract was then meticulously filtered through nº 7 filter paper (14 μm) (Qualy Comercial Eireli, Passos, MG, Brazil) using a funnel to remove any solid residues. The resulting filtered aqueous extract had a distinct light green coloration (data not shown).

2.2. Synthesis and characterization of nanoparticles

Silver nanoparticles (AgNPs) were synthesized using soybean leaf extract as the reducing and stabilizing agent. Silver nitrate ($AgNO_3$) (Sigma-Aldrich, St Louis, MO, USA) was selected as silver salt precursor and dissolved in type I water to a final concentration of 1 mmol L^{-1}. The AgNPs reaction syntheses were conducted using varying concentrations of plant extract: 0.78, 1.56, 3.12, 6.25, 12.5, and 25 mg of leaf mL^{-1}. The final suspensions were denoted as 1.56AgNPs, 3.12AgNP, 6.25AgNP, 12.5AgNP, and 25AgNP, respectively. The stock aqueous extract was diluted to these final concentrations, mixed with $AgNO_3$ solution, and then incubated at 65°C for 2.5 h. The resulting AgNPs were preserved in a polypropylene tube at 4°C in the dark for further physical-chemical characterization and testing of biological activity.

To characterize the nanoparticles, an absorbance curve was generated by collecting measurements from a UV-Vis spectrophotometer (Shimadzu UV-1203, Kyoto, Japan) across a wavelength range of 350 to 550 nm for each reaction synthesis. The peak with the highest intensity indicated the presence of the surface plasmon resonance (SPR) effect. The physical characterization of the AgNPs was then performed using dynamic light scattering (DLS) and electrophoretic mobility techniques on a ZetaSizer Nano ZS (Malvern Instruments, Worcestershire, United Kingdom), equipped with a He-Ne laser operating at 633 nm. This methodology facilitated the determination of several parameters, including the hydrodynamic diameter (HD) of the particles, the size distribution of the particle subpopulations evaluated by the polydispersity index (PdI), and the electrophoretic mobility expressed as Zeta potential. The assessments of HD, PdI, and Zeta potential were performed in triplicates, with the measurements automated and the scattering angle set at 173° at 25°C. Moreover, the reaction syntheses and the measurements of HD, PdI, and Zeta potential of AgNPs were repeated three times to confirm reproducibility. The data generated were processed using ZetaSizer software developed by Malvern Instruments.

The identification of functional groups in the soybean leaf extract that might contribute to the reduction, capping, and stabilization process of AgNPs was performed using Fourier-transform infrared spectroscopy (FTIR). FTIR spectra were obtained in potassium bromide (KBr) tablet and in the total attenuated total reflectance (ATR) mode using a Vertex 70 spectrometer (Bruker Corporation, Billerica, Massachusetts, United State), outfitted with an ATR configuration specifically tailored for the samples. The samples were deposited onto a diamond crystal and analyzed within a spectral range of 4000 to 350 cm^{-1}, at a resolution of 4 cm^{-1} with a total of 32 scans. The data collected were then acquired and analyzed using OPUS software v7.2 (Bruker Corporation).

2.3. P. brachyurus culture

The culture of the root lesion nematode, *P. brachyurus*, originating from the *Pratylenchus* culture collection of the University of Brasília, was conducted in the Department of Phytopathology, Brasília, Federal District, Brazil. The population was collected from naturally infected soybean plants harvested in a commercial area in the municipality of Luziânia, Goiás, in the Central region of Brazil. The nematode population was propagated in soybean plants growing within a controlled greenhouse environment at 25°C ± 3°C.

To confirm the species of the population, nematodes were extracted from the roots of soybean plants cultivated in the greenhouse. The extraction of nematodes was carried out using the methodology described by [33], followed by molecular, morphological, and morphometric characterization of specimens. For the molecular characterization, DNA was extracted from the *Pratylenchus* specimens using the DNeasy Blood and Tissue Kit (Qiagen). A pair of species-specific primers (18S-F and ACM7-R) designed to detect *P. brachyurus* was used, and the PCR process was accomplished as described by [34].

 doi:10.20944/preprints202311.0514.v1

For a detailed morphological and morphometric assessment, semi-permanent microscopy slides containing ten adult females were meticulously prepared. Various anatomical structures were studied, including body length (L), stylet length (ST), stylet bulb diameter (ØSTB), stylet bulb length (STB), tail length (T), esophagus length (ESO), distance from vulva to anus (VA), largest body diameter (ØL), body diameter at the anus (ØLA), body diameter at the vulva (ØLV), percentage distance of the vulva from the anterior end (V), and the overlap length of the esophageal glands (EG). Additionally, the De Man indices were also calculated: a (ratio of body length to largest body diameter), b (ratio of body length to esophagus length), c (ratio of body length to tail length), and c′ (ratio of tail length to tail diameter at anus height). The data were statistically analyzed using descriptive statistics, such as mean and standard deviation. The nematodes were classified according to the identification keys of [3] using a Leica DM2500 optical microscope (Leica, Wetzlar, Germany).

For all bioassay experiments, the inoculum density was calibrated to ~1000 nematodes mL^{-1} using a Peters' counting chamber with the same optical microscope set to a 40× objective.

2.4. Direct exposure of P. brachyurus to 3.12AgNP and 6.25AgNP

This experiment assessed the inhibitory impact of AgNPs, synthesized using different leaf extract concentrations on the mobility of the root lesion nematode, *P. brachyrus*, in an *in vitro* setting. Two distinct formulations of AgNPs were prepared using 3.12 mg and 6.25 mg of leaves per mL and were termed 3.12AgNP and 6.25AgNP, respectively. These formulations were chosen based on their physicochemical attributes, which aligned with the requisite criteria for nanomaterials.

The experimental procedure involved exposing 1,000 nematodes to six varying concentrations (1, 10, 25, 50, 125, and 250 μmol L^{-1}) of both 3.12AgNP and 6.25AgNP formulations independently. The nematode-nanoparticle mixtures were incubated at room temperature for 48 h, after which they were transferred to Baermann funnels for an additional 48 h following the protocol outlined by [35]. Subsequently, live nematodes were harvested from the terminal container after a total incubation period of 96 h and quantified to evaluate the inhibitory effect under each treatment condition. Sterile water served as the control solution. The experiment was conducted with five experimental units, each represented by one funnel, and was replicated twice at varying time intervals. This resulted in two distinct experimental batches, with a total of ten funnels evaluated under each treatment condition.

The minimum inhibitory concentration (IC50 and IC90 values, which represent the concentrations required to inhibit 50% and 90% of nematicidal activity, respectively) was ascertained through the analysis of two replicates, followed by logistic regression to fit curves to the data. An analysis of variance (ANOVA) was performed on these values, with treatment means compared using Fisher's Least Significant Difference test at a significance level of $\alpha = 0.05$.

2.5. AgNP effects on soybean grown and nematode population in soil system

Only the AgNP and concentrations that exhibited the highest nematicidal efficacy in preliminary *in vitro* mobility studies were selected for *in vivo* testing. Initially, soybean seeds were sowed in bags filled with a sterilized mixture of soil, sand, and Bioplant® commercial substrate, mixed in a 1:1:1 ratio. Upon reaching the V2 stage, the rhizosphere of each soybean plant was inoculated with a 1 mL suspension containing 1000 individuals of *P. brachyurus*. Three days after nematode inoculation, a 1 mL dose of the green-synthesized 6.25AgNP was applied to the soil surrounding the rhizosphere. The *in vivo* nematicidal efficacy of AgNPs was then assessed through two separate experiments, using application timings and concentrations derived from prior *in vitro* trials.

In the first experiment, a single dose of green-synthesized 6.25AgNP was administered at concentrations of 125 and 250 μmol L^{-1}. The second experiment involved a single dose of 6.25AgNP at 500 μmol L^{-1} and two subsequent doses at 250 μmol L^{-1}, spaced a month apart. Control treatments consisted of water applications. Throughout the experiment, plants were housed in a greenhouse maintained at a temperature of 25 ± 3°C for 80 days.

Following 80 days of nanoparticle application, various plant metrics were evaluated, including plant height, shoot weight, leaf count, root weight, nematodes per gram of root, and the nematode

 doi:10.20944/preprints202311.0514.v1

reproduction factor (RF) for each treatment. The RF was calculated based on the contrast between the final population (Pf) and initial population (Pi), following the methodology proposed by [36]. Nematode data per gram of root underwent an analysis of variance (ANOVA), with Fisher's least significant difference being calculated to a significance level of P=0.05 for treatment comparisons. Each treatment was composed of eight replicates with a single soybean plant in a 1 L pot. All infection sets were conducted twice at varying intervals.

2.6. Transmission Electron Microscopy (TEM) and Scanning Electron Microscopy (SEM)

To determine the average dry size of the most effective AgNPs and investigate their effects on nematode cuticles, a two-pronged microscopy approach was employed: Transmission Electron Microscopy (TEM) for particle analysis and Scanning Electron Microscopy (SEM).

In the first stage, the AgNPs were diluted in water and dispersed onto copper grids for TEM analysis using a JEOL 1011 microscope. The particle diameters were precisely measured using the ImageJ software, and the resultant size distribution curve was plotted using R software. For the SEM analysis, nematodes were submerged in AgNPs suspension for 24 h, rinsed with water, and then fixed in Karnovsky's solution (2% glutaraldehyde and 2% paraformaldehyde) buffered with 0.05 M sodium cacodylate at pH 7.2) for 12 h [37]. The nematodes were washed three times with 0.05 M sodium cacodylate and post-fixed with osmium tetroxide for 1 h. Subsequently, they were rinsed with distilled water and dehydrated through a sequential acetone series (50%, 70%, 90%, and twice at 100% concentrations). After dehydration, the samples were subjected to critical point drying using a Balzers CPD 030 with carbon dioxide as the transition fluid and mounted on supports adorned with carbon adhesive tape. The final step involved gold sputter coating using a Leica EM SCD 500, after which the samples were ready for SEM analysis on a JEOL JSM-7001F microscope. During each solution disposal stage, the material in 1.5 mL tubes was centrifuged at 2500 g for 3 min to ensure thorough separation.

3. Results

3.1. Optical and physical-chemical characterization of silver nanoparticles

Two rapid methods were used to monitor the successful formation of AgNPs: the transition of the suspension's color from yellow to brownish upon mixing the aqueous leaf extract with $AgNO_3$ solution and the emergence of peaks at a wavelength of approximately 425 nm in spectrophotometric analyses. Optical properties revealed that free silver ions (Ag^+), extracts (E), and the lowest concentration of the extract (1.56 mg of leaf mL^{-1}) mixed with $AgNO_3$ did not induce any color changes in the solution. On the other hand, all other reaction media containing various concentrations of the leaf soybean extract and $AgNO_3$ exhibited a color transition from yellow to brown, suggesting the formation of nanoparticles (Figure 1). Absorbance spectra were measured in the visible region of 350-550 nm using UV-Vis spectroscopy (Figure 2a). Absorbance peaks in the range of 410-430 nm were exclusively detected in the 3.12AgNP and 6.25AgNP suspensions, confirming the formation of AgNPs. Notably, the absorbance of these nanoparticles varied, with higher values being associated with higher leaf extract concentrations in the reaction. A reduced absorbance peak was observed in the 12.5AgNP and 25AgNP. No such peaks were identified in the other synthesis reactions, implying the lack of a SPR effect.

Preprints (www.preprints.org) | NOT PEER-REVIEWED | Posted: 8 November 2023 doi:10.20944/preprints202311.0514.v1

Figure 1. Reaction tubes containing suspensions of AgNPs, synthesized using varying concentrations of soybean leaf aqueous extract: 25, 12.5, 6.25, 3.12, 1.56, and 0.78 mg mL^{-1}, respectively.

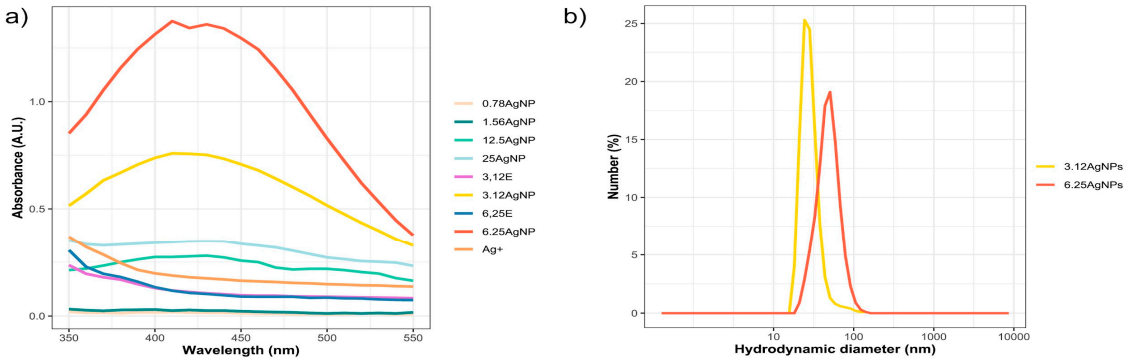

Figure 2. (**a**) Visible absorbance curves of AgNPs and extracts (E) obtained by green synthesis with soy leaf aqueous extract obtained at 65°C for 2.5 h. (**b**) Hydrodynamic diameter dispersion of AgNPs synthesized using 3.12 (3.12AgNPs) and 6.25 mg mL^{-1} of soybean leaf aqueous extract (6.25AgNPs).

The physical characteristics of the nanoparticles synthesized were analyzed using DLS and electrophoretic mobility. The 12.5AgNP and 25AgNP exhibited high HD (>450 nm) and expressive precipitation, therefore the possible nematicide activities of these nanoparticles were not evaluated. Otherwise, the 3.12AgNP and 6.25AgNP had an HD of 104.4 ± 2.4 nm and 73.5 ± 1.5 nm, respectively (Table 1). They exhibited a homogeneous size distribution, forming a uniformly singular population (Figure 2b). The concentration of the extract appeared to influence nanoparticle size, but the PdI and Zeta potential values were similar across both concentrations. The extract concentrations tested resulted in a relatively low PdI ranging from 0.23 ± 0.01 to 0.22 ± 0.02 (Table 1). The AgNPs exhibited a negative Zeta potential, ranging from -25.1 ± 0.5 to -23.3 ± 0.2 mV (Table 1). These values indicated that the AgNPs possess moderate colloidal stability due to sufficient mutual electrostatic repulsion to maintain suspension stability. No differences in size, PdI, and Zeta potential were observed among the three reaction syntheses in both concentrations of the leaf extract (Table 1).

Table 1. Physicochemical characteristic of the AgNPs synthesized with 3.12 (3.12AgNP) and 6.25 (6.25AgNP) mg mL^{-1} of soy leaf aqueous extract obtained by dynamic light scattering for obtaining the hydrodynamic diameter, polydispersity index (PdI), and Zeta potential synthesized three times.

	First synthesis			Second synthesis			Third synthesis		
Nanoparticles	**Size (d.nm)**	**PdI**	**Zeta Potential (mV)**	**Size (d.nm)**	**PdI**	**Zeta Potential (mV)**	**Size (d.nm)**	**PdI**	**Zeta Potential (mV)**
Ag+	64.7±4.3	0.57±0.04	-19.1±1.3	-	-	-	-	-	-

Preprints (www.preprints.org) | NOT PEER-REVIEWED | Posted: 8 November 2023 doi:10.20944/preprints202311.0514.v1

3.12AgNP	104.3±2.4	0.23±0.01	-25.1±0.5	101.1±3.4	0.19±0.01	-28.1±0.5	113.3±1.7	0.22±0.02	-20.2±1.4
6.25AgNP	73.5±1.5	0.22±0.02	-23.3±0.2	70.2±2.2	0.20±0.03	-23.3±0.2	79.1±1.8	0.19±0.05	-19.7±2.1

Functional groups in biomolecules from soybean leaf extract, potentially involved in the reduction of Ag^{+} and synthesis of 3.12AgNP and 6.25AgNP, were investigated using FTIR measurements. The absorbance bands identified in the spectra of the soybean extract were the same in both synthesis and located at 3449, 2920, 2851, 1637, 1461, 1384, 1032, and 461.8 cm^{-1} (Figure 3). Different concentrations of soybean leaf extract resulted in the detection of the same elements in the FTIR profile, with extracts containing 6.25 mg mL^{-1} exhibiting higher intensity for all peaks. Multiple peaks were observed in the analysis, which are described according to [38]: the peak at 3449 cm^{-1} corresponds to the stretching vibration of hydroxyl (OH) groups, commonly found in alcohols and phenols; the peaks at 2920 cm^{-1} and 2851 cm^{-1} are indicative of the vibration of aliphatic C-H bonds, typical in alkanes and alkyl groups; the peak at 1637 cm^{-1} is associated with an amide absorption band, suggesting the presence of peptide bonds in proteins; the peak at 1461 cm^{-1} is related to methyl groups; the peak at 1384 cm^{-1} is associated with various types of bonds, including C-H bonds in alkenes or ketones; the peak at 1032 cm^{-1} indicates a C-O band, characteristic of esters, alcohols, and other functional groups; lastly, the peak at 461.8 cm^{-1} is related to vibrations in metal bonds or bending modes in complex molecules.

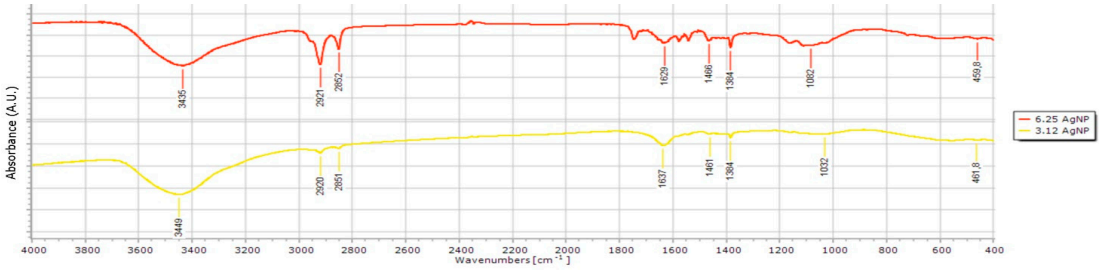

Figure 3. Fourier-transform infrared spectroscopy (FTIR) spectra of AgNPs synthesized using 3.12 (3.12AgNPs; yellow line) and 6.25 mg mL^{-1} soybean leaf aqueous extract (6.25AgNPs; red line).

3.2. In vitro and in vivo nematicidal activity of AgNPs

The *P. brachyurus* specimens were identified using PCR amplification with the species-specific primers 18S-F/ACM7-R and morphological analysis. The PCR process yielded a single fragment approximately 270 bp in length (data not shown), confirming the identification of *P. brachyurus* [34]. All morphological and morphometric measurements also indicated the species *P. brachyurus* (Table S1). Females exhibited body lenghts and widths ranging from 534.67-577.83 µm and 22.44-23.48 µm, respectively. The cephalic region is slightly offset from the main body, with the oral aperture featuring two distinct sclerotized lip annuli.The stylet is robust, with a length varying between 19.23 and 20.63 µm. It is distinguished by its tulip-shaped nodules, which maintain a relatively uniform width ranging from 4.35 to 4.68 µm. The medium bulb is robust and oval-shaped.

The length of the esophagus ranges from 81.47 to 87.09 µm. The esophageal glands, which overlap the intestine on the ventral and lateral sides, measure about 52.62 ± 1.14 µm. The vulva is located 452 to 482 µm from the anterior end, accounting for approximately 82.62% to 86.50% of the total body length. The reproductive system is monodelphic-prodelphic, with a non-functional spermatheca. The tail shape varies from club-shaped to truncated to conical, with a length of 28.56 to 31.76 µm. Males were not found (Figure S1).

After identifying the nematodes, the effects of different concentrations of AgNPs on their mobility and mortality were tested both *in vitro* and *in vivo*, respectively. After incubating the *P. brachyurus* specimens with 3.12AgNP and 6.25AgNP for 48 h, the nanoparticles significantly inhibited

Preprints (www.preprints.org) | NOT PEER-REVIEWED | Posted: 8 November 2023 doi:10.20944/preprints202311.0514.v1

the nematode mobility at concentration of 25 µmol L^{-1} or higher, compared to the control ($P < 0.05$) (Figure 4a-d). In one experiment, 6.25AgNP was more effective at high concentrations (125 and 250 µmol L^{-1}) (Figure 4c) ($P < 0.05$). Although both AgNPs had nematotoxic effects, a sigmoidal logistic curve was constructed and IC50 and IC90 were calculated to determine which nanoparticle was most toxic to the phytonematode.

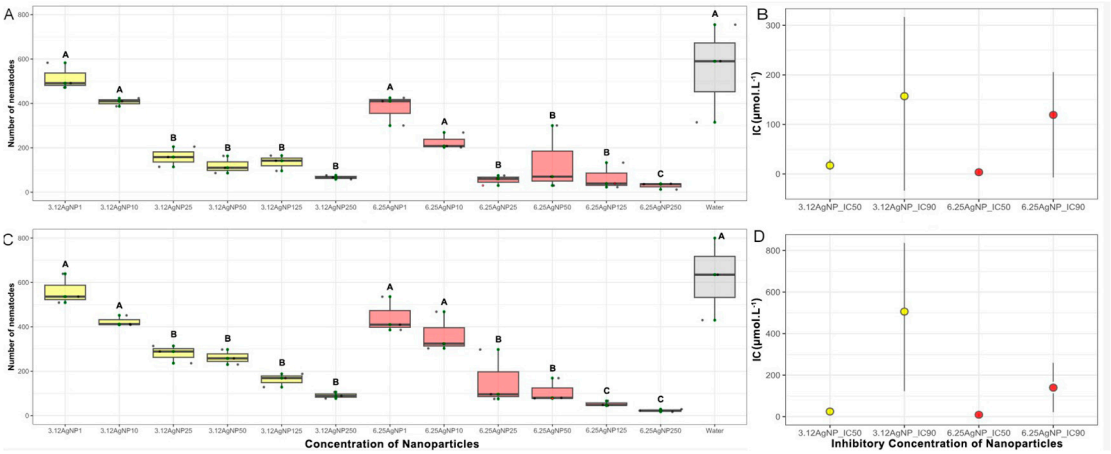

Figure 4. Six different concentrations (1, 10, 25, 50, 125, and 250 µmol mL^{-1}) of the AgNPs synthesized with 3.12 (3.12AgNP) and 6.25 mg mL^{-1} of aqueous soy leaf extract (6.25AgNP) in contact with *Pratylenchus brachyurus* specimens at room temperature for 48 h in first (**a**) and second (**c**) *in vitro* experiments. IC50 and IC90 values and confidence interval (bar) of AgNPs of treatment against *P. brachyurus* in first (**b**) and second (**d**) *in vitro* experiments. 3.12AgNP and 6.25AgNPs are represented by yellow and red color bars, respectively. The application of water was used as control represented by a gray color bar.

A sigmoidal logistic curve was fitted to the nematicidal effect progress with an R^2 value above 0.90, and the SE values were low, indicating a good model fit to the data in both experiments. Based on the logistic curves, IC50 and IC90 values were calculated, and the lowest values were found for 6.25AgNPs, with IC50 values ranging from 3.66 (0.85–8.19) to 9.6 (0.68–12.9) µmol L^{-1}, and IC90 of 119.29 (6.93–205.52) to 140.09 (22.35–212.53) µmol L^{-1}. This compared to an IC50 range of 17.21 (8.65-28.77) to 25.18 (13.65-36.71) and an IC90 range of 157.02 (33.66-316.70) to 506.45 (123.33-836.26) for 3.12AgNPs (Table 2; Figure 4b and 4d). Because 6.25AgNPs was the most effective in inhibiting the mobility of *P. brachyurus in vitro*, only this AgNP at the concentrations of 125 and 250 µmol L^{-1} was tested in the *in vivo* to investigate its potential to interfere with multiplication and/or lead to nematode death.

Table 2. IC50 and IC90 values and confidence interval (parentheses) of AgNPs of treatment against *Pratylenchus brachyurus* in first and second *in vitro* experiments.

Nanoparticles	Experiment_1	Experiment_2
3.12AgNP_IC50	17.21 (8.65-28.77)	25.18 (13.65-36.71)
6.25AgNP_IC50	3.66 (0.85-8.19)	9.6 (0.68-12.9)
3.12AgNP_IC90	157.02 (33.66-316.7)	506.45 (123.33-836.26)
6.25AgNP_IC90	119.29 (6.93-205.52)	140.09 (22.35-212.53)

In the first set of *in vivo* experiments, the application of 6.25AgNP at a concentration of 125 and 250 µmol L^{-1} differed from the control in the number of nematodes per gram of root by up 62%, with no phytotoxicity observed in either experiment ($P < 0.05$) (Figure 5a- b). Otherwise, the FRs were greater than 1, indicating that the nematode population multiplied in the root when 6.25AgNP was applied once at a concentration of 125 and 250 µmol L^{-1}. To try to inhibit the phytonematode multiplication, we repeated the experiment by applying 6.25AgNP at a concentration of 250 µmol L^{-1} three days after nematode inoculation and again after 30 days. We also evaluated the application of

Preprints (www.preprints.org) | NOT PEER-REVIEWED | Posted: 8 November 2023 doi:10.20944/preprints202311.0514.v1

nanoparticles once at a concentration of 500 µmol L^{-1} three days after inoculation. Increasing the number of nanoparticle applications and using a higher concentration enhanced the *in vivo* nematicidal activity against *P. brachyurus*, resulting in an FR< 1 in both treatments. Furthermore, two applications of 6.25AgNP at a concentration of 250 µmol L^{-1} were more effective than one application of AgNPs at a concentration of 500 µmol L^{-1} ($P < 0.05$). No statistical differences were observed in plant height, shoot weight, leaf count, or root weight with the application of different concentrations of nanoparticles in the soil (data not shown).

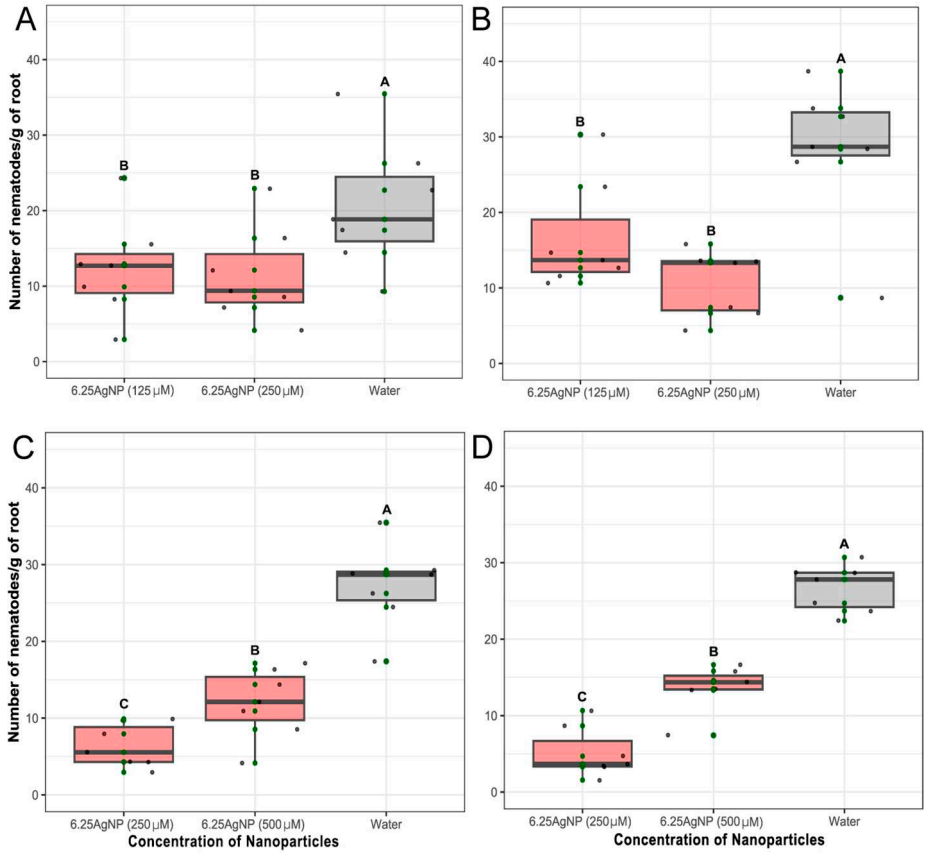

Figure 5. (**a-b**) Number of *Pratylenchus brachyurus* specimens/gram of soybean root treated with one application of 6.25 mg mL^{-1} of soy leaf aqueous extract (6.25AgNP) at a concentration of 125 µmol L^{-1} and 250 µmol L^{-1}. (c-d) Number of nematode/gram of soybean root treated with one application of 6.25 mg mL^{-1} of soybean leaf aqueous extract (6.25AgNP) at a concentration of 500 µmol L^{-1} and two application of 250 µmol L^{-1} spaced one month apart. The application of water was used as control. The number of nematodes was scored after 80 days of nematode inoculation. Mean of number of nematodes/gram of soybean root was calculated using data from eight repetitions. Error bars represent the SE calculated from eight repetitions. Treatments are indicated in the X-axis.

3.3. 6.25AgNP dry size and mode of action on phytonematodes

To better understand the dry diameter size and shape of the synthesized 6.25AgNP, as well as their improved physicochemical properties and nematicidal activity, TEM analysis was employed. This analysis revealed the presence of spherical AgNPs with an average size of 11.89 ± 9.28 nm. Some degree of agglomeration was observed, accompanied by moderate size variations (Figure 6a-b).

Preprints (www.preprints.org) | NOT PEER-REVIEWED | Posted: 8 November 2023 doi:10.20944/preprints202311.0514.v1

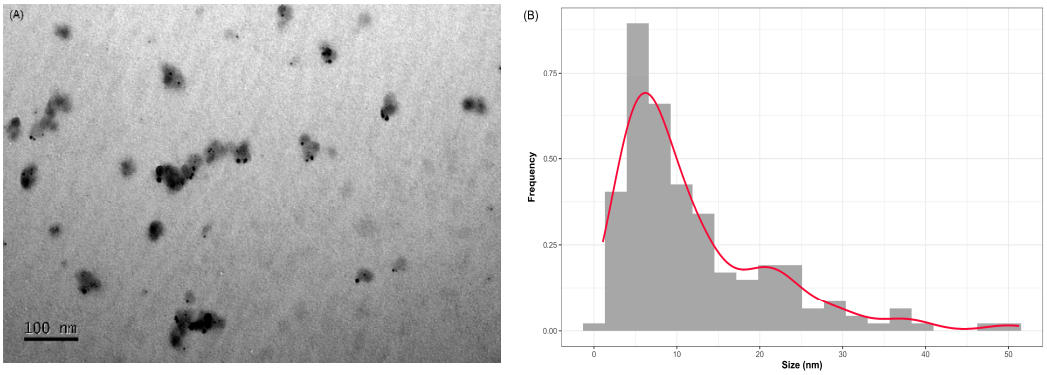

Figure 6. (**a**) Images obtained by transmission electron microscopy (TEM) of AgNPs synthesized using 6.25 mg mL-1 of soybean leaf aqueous extract (6.25AgNPs) of soybean leaf aqueous extract and (**b**) particles size distribution for 6.25AgNPs in dry condition.

Examination of SEM images suggests that the 6.25AgNPs initially adhere to the nematode cuticle. However, no discernible alterations in the cuticle were detected during the exposure period to AgNPs (Figure 7a-d).

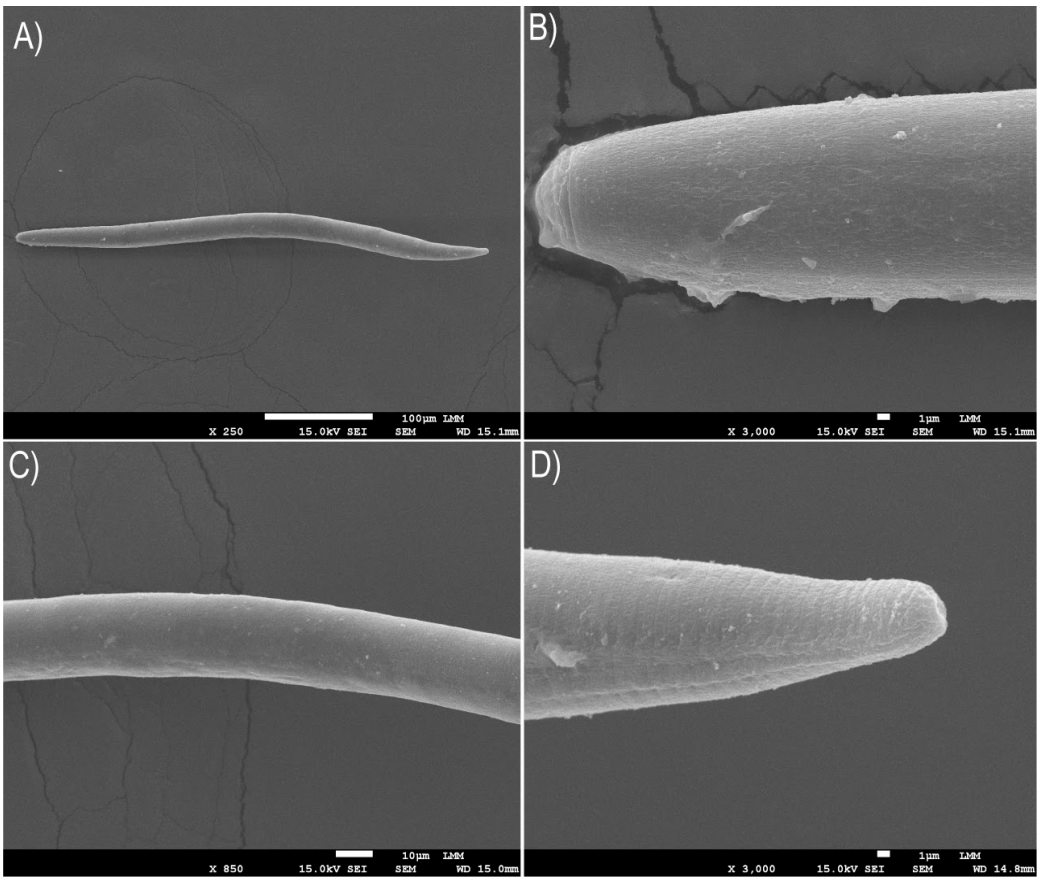

Figure 7. Scanning electron microscopy (SEM) images were taken after exposing the *Pratylenchus brachyurus* specimens in a 250 µmol L^{-1} solution of AgNPs (synthesized using 6.25 mg mL^{-1} of soy leaf aqueous extract, termed 6.25AgNPs) for a period of 48 h. The images depict various parts of *P. brachyurus* adult: (**a**) the body, (**b**) labial region, (**c**) median region, and (**d**) tail terminus.

4. Discussion

Modern agricultural research aims to promote sustainable practices that reduce reliance on external inputs and foster biodiversity. This involves employing non-polluting techniques and

 doi:10.20944/preprints202311.0514.v1

repurposing all by-products. Our study delves into this concept, demonstrating the use of lesser-utilized soybean by-products as reliable agents to reduce silver ions, generating AgNPs. These nanoparticles provide an eco-friendly solution to control the destructive phytonematode *P. brachyurus*, an important threat to tropical soybean crops. Using soybean leaf extract, we efficiently converted silver ions into spherical nanoparticles characterized by uniform distribution, low polydispersity, and hydrodynamic diameters ranging from 73 to 104 nm.

While previous research has explored the green synthesis of these nanoparticles through soybean leaf extract [31,32], our study investigated the reproducibility of the reaction synthesis at different intervals. We also evaluated how fluctuating extract concentrations affect the physical and biological attributes of the AgNPs. We confirmed AgNPs formation using leaf concentrations of 3.12 and 6.25 mg mL, evidenced by color changes and UV-Vis absorption peaks (410-430 nm), demonstrating the SPR effect. Additionally, we observed an increase in absorbance as the extract concentration in the reactions increased, as shown in Figure 2a. This enhanced absorbance, a manifestation of the SPR effect, could indicate alterations in the AgNPs' size, shape, composition, reduction yield, surface characteristics, or potential shifts in biological activity [39].

Our findings suggest that doubling the concentration of the leaf extract led to a decrease in AgNPs size while enhancing its effectiveness against *P. brachyurus*. However, concentrations lower than 3.12 mg and higher than 6.25 mg of extract per mL inhibited the reduction of silver ions, thereby preventing AgNPs formation. This was evidenced by either minimal absorbance peaks below 400 nm or the absence of formation of nanometric particles sized less than 100 nm. The presence and/or concentration of specific constituents within the soybean extract could either inhibit or promote AgNPs formation, as well affect their dimensions and form [40,41]. Achieving reproducible physicochemical properties of AgNPs presents a significant challenge, given that minor variations in plant growth conditions can alter the properties of secondary metabolites responsible for the reduction of silver ions [42–45]. A noteworthy point from our study is the observed absence of reproductive anomalies, which might be attributed to the uniform handling of the soybean leaves. These leaves were collected simultaneously and stored securely until utilized for reaction syntheses, ensuring consistency in the material used.

Various studies have highlighted a range of biomolecules pivotal in the formation and properties of nanoparticles, including polysaccharides, polyphenols, and alcohols [46–48]. Building on this knowledge, we further investigated the specific functional groups in soybean leaves that facilitate the reduction of Ag^{+} ions to Ag^{0}. We employed FTIR analysis to provide useful insights into the mechanisms underlying AgNPs synthesis mediated by soybean leaf extracts. Our results showcased the complex and multifunctional nature of compounds derived from soybean aqueous extracts, demonstrating a variety of biomolecules functional groups that can facilitate the reduction of metal ions. The presence of signals corresponding to alcohols and phenols, along with amide absorption bands, indicates the likely involvement of phenolic acids, and polysaccharides in the reduction process. This is consistent with earlier research that emphasized the expressive silver ion binding capacities of amino acids and polysaccharides present in soybean leaves [49]. Other studies have proposed that agents such as flavonoids and isoflavones [50,51], as well as soluble soybean polysaccharides [52–54], could also act as potential reducing agents in this process.

Although our synthesized AgNPs demonstrated varied toxicity towards *P. brachyurus*, they did not cause any negative effects on soybean plants. In a broader context, different studies suggest that exposure for up to 3 days at 100-800 μmol L^{-1} is needed to achieve noticeable reductions in phytonematode mobility or mortality [55–57]. In our experiments, we observed that a 48 h exposure with AgNPs was required to neutralize over 50% of the nematode population's mobility (IC50) at concentrations ranging from 3.66 to 25.18 μmol L^{-1}. Our findings align with [58], who reported similar effective concentrations of marine algae-derived AgNPs against tomato-infecting nematodes. Notably, even at identical concentrations, there were discernible differences in the effectiveness between the 3.12AgNPs and 6.25AgNPs treatments. The latter AgNPs demonstrated superior results. This can be attributed to the consensus that smaller nanoparticles, due to their increased surface area, display enhanced reactivity and efficacy [59,60]. Moreover, *in vitro* experiments revealed a greater

 doi:10.20944/preprints202311.0514.v1

reduction in nematode mobility when exposed to AgNP concentrations of 125 and 250 μmol L^{-1}, especially to 6.25AgNP.

These promising *in vitro* results were not replicated in *in vivo* trials with *P. brachyurus*. In the soybean rhizospheres, nematode proliferation at concentration of 125 and 250 μmol L^{-1} reduced the number of nematodes in the root comparable to the control group. However, surprisingly, both concentrations resulted in a reproduction factor (RF) greater than 1, indicating nematode reproduction even after the application of AgNPs. The contrast between *in vitro* and *in vivo* findings highlights the complex interplay of AgNPs behavior within the soil environment. This complexity can be attributed to various factors, including AgNPs absorption by plant roots and their attachment to soil particles, resulting in dynamic nanoparticle distributions in the vicinity of the roots [61], and their interactions with the multifaceted rhizosphere microbial community [62]. Such behavior, highlighted in recent studies like that of [63], points to the intricate challenge of predicting nanoparticle effects in natural settings and underscores the need for extensive research to unravel the underlying mechanisms at play.

Another contributing factor could be that AgNPs show diminished effectiveness, possibly because of the nematodes' ability to evade, especially in mobile species like *Pratylenchus* species, or the lack of correlation between the dose to inhibit mobility and mortality. Importantly, the discrepancy in outcomes was lessened when either a single high-dosage application of 500 μmol L^{-1} was used, and mainly when 250 μmol L^{-1} was administered repeatedly in a second assay. The repeated exposure to the AgNPs may cause a cumulative or enhanced effect on the nematode population, disrupting their development or survival over time. This paves the way for further exploration into optimizing dosage strategies to harness the nematicidal potential of AgNPs.

An in-depth analysis using SEM depicted AgNPs accumulation on the nematode cuticle, albeit without apparent immediate alterations to the cuticle, highlighting the need for further research to understand the prolonged influence of AgNPs on nematode physiology and behavior. Previous studies have suggested that AgNPs affect phytonematodes through complex and diverse cellular mechanisms [64]. AgNPs have the potential to induce adverse effects, including germ cell death, reproductive problems, reduced life expectancy, and genetic damage across generations, as nematodes internalize these particles [65–68].

In accordance with environmental regulations, it's worth noting that regulatory agencies, including the Brazilian Ministry of Health has established a permissible level for elemental silver in drinking water at 50 μg mL^{-1} [69]. In our study, the applied silver concentrations consistently remained below this threshold, measuring at 0.084 μg mL^{-1}. Our findings underscore the relevance of sustainable nematode management in soybean cultivation. Green-synthesized AgNPs exhibit remarkable nematicidal action against *P. brachyurus*, positioning them as a viable alternative to traditional chemical-based solutions. Their eco-friendliness further accentuates their appeal, alleviating environmental pollution concerns tied to conventional methods.

The potential of AgNPs as a nematode control strategy necessitates further exploration. Elucidating the long-term effects on nematode physiology and their reproductive, developmental, and behavioral aspects is vital. Understanding AgNPs' nematicidal action and soil AgNPs absorbance can refine their field application and dosage. Assessing their impact on non-target organisms and soil health will ensure their safe and sustainable application in tropical soybean cultivation regions.

In essence, our study unveils the promise of green-synthesized AgNPs against *P. brachyurus* in soybean agriculture. They emerge as an environmentally conscious and sustainable tool against nematode infestations. This research contributes substantially to the broader understanding of AgNPs' biological capabilities and practical applications, marking a pivotal move towards greener nematode control solutions in the agricultural realm.

Supplementary Materials: The following supporting information can be downloaded at the website of this paper posted on Preprints.org. Figure S1: (**a**) Photomicrograph of *Pratylenchus brachyurus* females showcasing the sausage-shaped body with the vulva position indicated by an arrow. (**b**) The cephalic region slightly offset from the main body with the oral aperture featuring two distinct sclerotized lip annuli, a robust stylet, and tulip-shaped nodules. (**c**) Esophageal glands overlap the intestine ventrally and laterally with a robust medium bulb.

(**d**) The tail's morphology is characterized as club-shaped, truncated, and conical.; Table S1: Morphological and morphometric characterization of *Pratylenchus brachyurus:* overall body length (L), tail size (T), esophagus length (ESO), stylet length (ST), stylet bulb length (STB), diameter of stylet bulb (ØSTB), distance of vulva to anus (VA), largest body diameter (ØL), body diameter at anus height (ØLA), body diameter at vulva height (ØLV), % vulva from the anterior end (V; V%), length of overlap of esophageal glands (EG), a (relationship L/ØL), b (relationship L/ESO), c (relationship L/T) and c' (relationship T/ØLA). Data are means of 10 adult female's specimens.

Author Contributions: Conceptualization, T.R.S.; synthesis and characterization of AgNPs, L.S.O., and L.P.S.; *in vitro* and *in vivo* experiments, L.S.O., F.A.S.D., and T.R.A; nematode identification, F.A.S.D. and B.L.M.; microscopy experiments, L.L.F. and B.L.M.; FTIR analysis, B.L.M. and T.R.S.; formal analysis, L.S.O. and T.R.S.; funding acquisition, T.R.S. and L.P.S.; writing—original draft preparation, L.S.O. and T.R.S.; writing—review and editing, all authors. All authors have read and agreed to the published version of the manuscript.

Funding: This study was funded by the Fundação de Amparo à Pesquisa do Distrito Federal (FAPDF) through grant numbers 00193-00000783/2021-16 and 00193-001392/2016; Conselho Nacional de Desenvolvimento Científico e Tecnológico (CNPq) under grant numbers 421810/2021-1, 311825/2021-4, 307853/2018-7, 408857/2016-1, 306413/2014-0, and 563802/2010-3; Coordenação de Aperfeiçoamento de Pessoal de Nível Superior - Brasil (CAPES) under grant number 23038.019088/2009-58; and Empresa Brasileira de Pesquisa Agropecuária (Embrapa) under grant numbers no. 10.20.03.009.00.00, 23.17.00.069.00.02, 13.17.00.037.00.00, 21.14.03.001.03.05, 13.14.03.010.00.02, 12.16.04.010.00.06, 22.16.05.016.00.04, and 11.13.06.001.06.03. The authors extend their gratitude to CNPq for awarding scholarships to L.S.O., L.L.F., and F.A.S.D.

Acknowledgments: The author(s) would like to thank Prof. Sonia Maria de Freitas and Sonia Nair Báo for allowing the use of the dynamic light scattering (DLS) equipment in the Biophysics Laboratory, as well as the transmission electron microscope (JEOL 1011) and scanning electron microscopy (JEOL JSM-7001F) in the Microscopy and Microanalysis Laboratory at the University of Brasília, respectively. We also express our gratitude to Prof. Sebastião Willian da Silva for his assistance with the analyses using the Fourier-transform infrared spectroscopy (FTIR) equipment.

Conflicts of Interest: The authors declare no conflict of interest.

References

1. Lordello, L.G.E. *Nematóides Das Plantas Cultivadas*; Nobel: São Paulo, SP, Brazil, 1986.
2. Ferraz, L.; Brown, D. *Nematologia de Plantas: Fundamentos e Importância*; Norma Editora: Manaus, AM, Brazil, 2016; Vol. 1; ISBN 978-85-99031-26-1.
3. Castillo, P.; Vovlas, N. *Pratylenchus, Nematoda: Pratylenchidae: Diagnosis, Biology, Pathogenicity and Management*; Nematology monographs and perspectives; Brill: Leiden, 2007; ISBN 978-90-04-15564-0.
4. Goulart, A. Aspectos Gerais Sobre Nematóides das Lesões Radiculares (Gênero *Pratylenchus*). 2008. Availabe online: https://ainfo.cnptia.embrapa.br/digital/bitstream/CPAC-2010/30288/1/doc-219.pdf (accessed on 31 october 2023).
5. Vieira, P.; Maier, T.R.; Eves-van Den Akker, S.; Howe, D.K.; Zasada, I.; Baum, T.J.; Eisenback, J.D.; Kamo, K. Identification of Candidate Effector Genes of *Pratylenchus penetrans*. Mol. Plant Pathol. **2018**, 19, 1887–1907, doi:10.1111/mpp.12666.
6. Vovlas, N.; Troccoli, A. Histopathology of broad bean roots infected by the lesion nematode *Pratylenchus penetrans*. Nematol. Medit. **1990**, 18, 239–242.
7. Thompson, J.P.; Owen, K.J.; Stirling, G.R.; Bell, M.J. Root-Lesion Nematodes (*Pratylenchus thornei* and *P. neglectus*): A Review of Recent Progress in Managing a Significant Pest of Grain Crops in Northern Australia. Australas. Plant Pathol. **2008**, 37, 235, doi:10.1071/AP08021.
8. Bergeson, G.B. Concepts of Nematode—Fungus Associations in Plant Disease Complexes: A Review. Exp. Parasitol. **1972**, 32, 301–314, doi:10.1016/0014-4894(72)90037-9.
9. De Waele, D.; Elsen, A. Challenges in Tropical Plant Nematology. Annu. Rev. Phytopathol. **2007**, 45, 457–485, doi:10.1146/annurev.phyto.45.062806.094438.
10. Haegeman, A.; Jones, J.T.; Danchin, E.G.J. Horizontal Gene Transfer in Nematodes: A Catalyst for Plant Parasitism? Mol. Plant-Microbe Interactions **2011**, 24, 879–887, doi:10.1094/MPMI-03-11-0055.
11. Nicol, P.; Gill, R.; Fosu-Nyarko, J.; Jones, M.G.K. De Novo Analysis and Functional Classification of the Transcriptome of the Root Lesion Nematode, *Pratylenchus thornei*, after 454 GS FLX Sequencing. Int. J. Parasitol. **2012**, 42, 225–237, doi:10.1016/j.ijpara.2011.11.010.
12. Fosu-Nyarko, J.; Jones, M.G.K. Advances in Understanding the Molecular Mechanisms of Root Lesion Nematode Host Interactions. Annu. Rev. Phytopathol. **2016**, 54, 253–278, doi:10.1146/annurev-phyto-080615-100257.
13. Bridge, J. Nematode Management in Sustainable and Subsistence Agriculture. Annu. Rev. Phytopathol. **1996**, 34, 201–225, doi:10.1146/annurev.phyto.34.1.201.

14. Abd-Elgawad, M.M.M. Understanding Molecular Plant–Nematode Interactions to Develop Alternative Approaches for Nematode Control. Plants **2022**, 11, 2141, doi:10.3390/plants11162141.
15. Karuri, H. Root and Soil Health Management Approaches for Control of Plant-Parasitic Nematodes in Sub-Saharan Africa. Crop Prot. **2022**, 152, 105841, doi:10.1016/j.cropro.2021.105841.
16. Khan, F.; Shariq, M.; Asif, M.; Siddiqui, M.A.; Malan, P.; Ahmad, F. Green Nanotechnology: Plant-Mediated Nanoparticle Synthesis and Application. Nanomaterials **2022**, 12, 673, doi:10.3390/nano12040673.
17. Hassan, M.E.M.; Zawam, H.S.; Nahas, S.E.M.E.-; Desoukey, A.F. Comparison Study Between Silver Nanoparticles and Two Nematicides Against *Meloidogyne incognita* on Tomato Seedlings. Plant Pathol. J. **2016**, 15, 144–151, doi:10.3923/ppj.2016.144.151.
18. Hamed, S.M.; Hagag, E.S.; El-Raouf, N.A. Green Production of Silver Nanoparticles, Evaluation of Their Nematicidal Activity against *Meloidogyne javanica* and Their Impact on Growth of Faba Bean. Beni-Suef Univ. J. Basic Appl. Sci. **2019**, 8, 9, doi:10.1186/s43088-019-0010-3.
19. Mahmoud, W.M.; Abdelmoneim, T.S.; Elazzazy, A.M. The Impact of Silver Nanoparticles Produced by *Bacillus pumilus* as Antimicrobial and Nematicide. Front. Microbiol. **2016**, 7, doi:10.3389/fmicb.2016.01746.
20. Oluwatoyin, F.; Gabriel, O.; Olubunmi, A.; Olanike, O. Preparation of Bio-Nematicidal Nanoparticles of *Eucalyptus officinalis* for the Control of Cyst Nematode (*Heterodera sacchari*). J. Anim. Plant Sci. **2020**, 30, doi:10.36899/JAPS.2020.5.0134.
21. Mittal, A.K.; Chisti, Y.; Banerjee, U.C. Synthesis of Metallic Nanoparticles Using Plant Extracts. Biotechnol. Adv. **2013**, 31, 346–356, doi:10.1016/j.biotechadv.2013.01.003.
22. Razavi, M.; Salahinejad, E.; Fahmy, M.; Yazdimamaghani, M.; Vashaee, D.; Tayebi, L. Green Chemical and Biological Synthesis of Nanoparticles and Their Biomedical Applications. In Green Processes for Nanotechnology; Basiuk, V.A., Basiuk, E.V., Eds.; Springer International Publishing: Cham, 2015; pp. 207–235 ISBN 978-3-319-15460-2.
23. Hano, C.; Abbasi, B.H. Plant-Based Green Synthesis of Nanoparticles: Production, Characterization and Applications. Biomolecules **2021**, 12, 31, doi:10.3390/biom12010031.
24. Thummaneni, C.; Surya Prakash, D.V.; Golli, R.; Vangalapati, M. Green Synthesis of Silver Nanoparticles and Characterization of Caffeic Acid from *Myristica fragrans* (Nutmeg) against Antibacterial Activity. Mater. Today Proc. **2022**, 62, 4001–4005, doi:10.1016/j.matpr.2022.04.586.
25. Abbassy, M.A.; Abdel-Rasoul, M.A.; Nassar, A.M.K.; Soliman, B.S.M. Nematicidal Activity of Silver Nanoparticles of Botanical Products against Root-Knot Nematode, *Meloidogyne incognita*. Arch. Phytopathol. Plant Prot. **2017**, 50, 909–926, doi:10.1080/03235408.2017.1405608.
26. Danish, M.; Altaf, M.; Robab, M.I.; Shahid, M.; Manoharadas, S.; Hussain, S.A.; Shaikh, H. Green Synthesized Silver Nanoparticles Mitigate Biotic Stress Induced by *Meloidogyne incognita* in *Trachyspermum ammi* (L.) by Improving Growth, Biochemical, and Antioxidant Enzyme Activities. ACS Omega **2021**, 6, 11389–11403, doi:10.1021/acsomega.1c00375.
27. Duraisamy, K.; Palanisamy, S.; Premasudha, P.; Hafez, S. Nematicidal Activity of Green Synthesized Silver Nanoparticles Using Plant Extracts against Root-Knot Nematode *Meloidogyne incognita*. 2017, 27, 81–94.
28. Elkobrosy, D.; Al-Askar, A.A.; El-Gendi, H.; Su, Y.; Nabil, R.; Abdelkhalek, A.; Behiry, S. Nematocidal and Bactericidal Activities of Green Synthesized Silver Nanoparticles Mediated by *Ficus sycomorus* Leaf Extract. Life **2023**, 13, 1083, doi:10.3390/life13051083.
29. Heflish, A.A.; Hanfy, A.E.; Ansari, M.J.; Dessoky, E.S.; Attia, A.O.; Elshaer, M.M.; Gaber, M.K.; Kordy, A.; Doma, A.S.; Abdelkhalek, A.; et al. Green Biosynthesized Silver Nanoparticles Using *Acalypha wilkesiana* Extract Control Root-Knot Nematode. J. King Saud Univ. - Sci. **2021**, 33, 101516, doi:10.1016/j.jksus.2021.101516.
30. Kalaiselvi, D.; Mohankumar, A.; Shanmugam, G.; Nivitha, S.; Sundararaj, P. Green Synthesis of Silver Nanoparticles Using Latex Extract of *Euphorbia tirucalli*: A Novel Approach for the Management of Root Knot Nematode, *Meloidogyne incognita*. Crop Prot. **2019**, 117, 108–114, doi:10.1016/j.cropro.2018.11.020.
31. Vivekanandhan Biological Synthesis of Silver Nanoparticles Using *Glycine max* (Soybean) Leaf Extract: An Investigation on Different Soybean Varieties. J. Nanosci. Nanotechnol. **2009**, 9, doi:10.1166/jnn.2009.2201.
32. Hosamani, G.; Patil, R.R.; Benagi, V.I.; Chandrashekhar, S.S.; Nandihali, B.S. Synthesis of Green Silver Nanoparticles from Soybean Seed and Its Bioefficacy on *Spodoptera litura* (F.). Int. J. Curr. Microbiol. Appl. Sci. 2019, 8, 610–618, doi:10.20546/ijcmas.2019.809.073.
33. Coolen, W.A.; D'Herde, C.J. A Method for the Quantitative Extraction of Nematodes from Plant Tissue **1972**.
34. Machado, A.C.Z.; Ferraz, L.C.C.B.; de Oliveira, C.M.G. Development of a Species-Specific Reverse Primer for the Molecular Diagnostic of *Pratylenchus brachyurus*. Nematropica **2007**, 37, 10.
35. Flegg, J.J.M. Extraction of *Xiphinema* and *Longidorus* Species from Soil by a Modification of Cobb's Decanting and Sieving Technique. Ann. Appl. Biol. **1967**, 60, 429–437, doi:10.1111/j.1744-7348.1967.tb04497.x.
36. Oostenbrink, M. Major Characteristics of the Relation between Nematodes and Plants. Medelingen Van De landbouwhogeschool Te Wageningen 1966, 1–46.

37. Karnovsky, M. A Formaldehyde-Glutaraldehyde Fixative of High Osmolality for Use in Electron Microscopy. J Cell Biol 1965, 27.
38. Pavia, D.L.; Lampman, G.M.; Kriz, G.S. *Introduction to Spectroscopy: A Guide for Students of Organic Chemistry*; 3rd ed.; Harcourt College Publishers: Fort Worth, 2001; ISBN 978-0-03-031961-7.
39. Santiago, T.R.; Bonatto, C.C.; Rossato, M.; Lopes, C.A.P.; Lopes, C.A.; G Mizubuti, E.S.; Silva, L.P. Green Synthesis of Silver Nanoparticles Using Tomato Leaf Extract and Their Entrapment in Chitosan Nanoparticles to Control Bacterial Wilt. J. Sci. Food Agric. **2019**, 99, 4248–4259, doi:10.1002/jsfa.9656.
40. Roy, N.; Gaur, A.; Jain, A.; Bhattacharya, S.; Rani, V. Green Synthesis of Silver Nanoparticles: An Approach to Overcome Toxicity. Environ. Toxicol. Pharmacol. **2013**, 36, 807–812, doi:10.1016/j.etap.2013.07.005.
41. Abboud, Z.; Vivekanandhan, S.; Misra, M.; Mohanty, A.K. Leaf Extract Mediated Biogenic Process for the Decoration of Graphene with Silver Nanoparticles. Mater. Lett. **2016**, 178, 115–119, doi:10.1016/j.matlet.2016.04.120.
42. Akula, R.; Ravishankar, G.A. Influence of Abiotic Stress Signals on Secondary Metabolites in Plants. Plant Signal. Behav. **2011**, 6, 1720–1731, doi:10.4161/psb.6.11.17613.
43. Zhang, Y.; Qi, G.; Yao, L.; Huang, L.; Wang, J.; Gao, W. Effects of Metal Nanoparticles and Other Preparative Materials in the Environment on Plants: From the Perspective of Improving Secondary Metabolites. J. Agric. Food Chem. **2022**, 70, 916–933, doi:10.1021/acs.jafc.1c05152.
44. Yang, L.; Wen, K.-S.; Ruan, X.; Zhao, Y.-X.; Wei, F.; Wang, Q. Response of Plant Secondary Metabolites to Environmental Factors. Molecules **2018**, 23, 762, doi:10.3390/molecules23040762.
45. Mohammadlou, M.; Maghsoudi, H.; Jafarizadeh-Malmiri, H. A Review on Green Silver Nanoparticles Based on Plants: Synthesis, Potential Applications and Eco-Friendly Approach. Int. Food Res. J. **2016**, 23, 446.
46. Lee, J.H.; Ju, J.E.; Kim, B.I.; Pak, P.J.; Choi, E.-K.; Lee, H.-S.; Chung, N. Rod-Shaped Iron Oxide Nanoparticles Are More Toxic than Sphere-Shaped Nanoparticles to Murine Macrophage Cells: Toxicity of Rod and Sphere Iron Oxide Nanoparticles. Environ. Toxicol. Chem. **2014**, 33, 2759–2766, doi:10.1002/etc.2735.
47. Ahmed, S.; Ahmad, M.; Swami, B.L.; Ikram, S. A Review on Plants Extract Mediated Synthesis of Silver Nanoparticles for Antimicrobial Applications: A Green Expertise. J. Adv. Res. **2016**, 7, 17–28, doi:10.1016/j.jare.2015.02.007.
48. Mustapha, T.; Misni, N.; Ithnin, N.R.; Daskum, A.M.; Unyah, N.Z. A Review on Plants and Microorganisms Mediated Synthesis of Silver Nanoparticles, Role of Plants Metabolites and Applications. Int. J. Environ. Res. Public. Health **2022**, 19, 674, doi:10.3390/ijerph19020674.
49. Kumar Petla, R.; Vivekanandhan, S.; Misra, M.; Kumar Mohanty, A.; Satyanarayana, N. Soybean (*Glycine max*) Leaf Extract Based Green Synthesis of Palladium Nanoparticles. J. Biomater. Nanobiotechnology **2012**, 03, 14–19, doi:10.4236/jbnb.2012.31003.
50. Sathishkumar, P.; Gu, F.L.; Zhan, Q.; Palvannan, T.; Mohd Yusoff, A.R. Flavonoids Mediated 'Green' Nanomaterials: A Novel Nanomedicine System to Treat Various Diseases – Current Trends and Future Perspective. Mater. Lett. **2018**, 210, 26–30, doi:10.1016/j.matlet.2017.08.078.
51. Marslin, G.; Siram, K.; Maqbool, Q.; Selvakesavan, R.; Kruszka, D.; Kachlicki, P.; Franklin, G. Secondary Metabolites in the Green Synthesis of Metallic Nanoparticles. Materials **2018**, 11, 940, doi:10.3390/ma11060940.
52. Park, Y.; Hong, Y.N.; Weyers, A.; Kim, Y.S.; Linhardt, R.J. Polysaccharides and Phytochemicals: A Natural Reservoir for the Green Synthesis of Gold and Silver Nanoparticles. IET Nanobiotechnol. **2011**, 5, 69, doi:10.1049/iet-nbt.2010.0033.
53. Liu, J.; Dong, Y.; Ma, Z.; Rao, Z.; Zheng, X.; Tang, K. Soluble Soybean Polysaccharide/Carrageenan Antibacterial Nanocomposite Films Containing Green Synthesized Silver Nanoparticles. ACS Appl. Polym. Mater. **2022**, 4, 5608–5618, doi:10.1021/acsapm.2c00635.
54. Ma, Z.; Liu, J.; Liu, Y.; Zheng, X.; Tang, K. Green Synthesis of Silver Nanoparticles Using Soluble Soybean Polysaccharide and Their Application in Antibacterial Coatings. Int. J. Biol. Macromol. **2021**, 166, 567–577, doi:10.1016/j.ijbiomac.2020.10.214.
55. Cromwell, W.A.; Yang, J.; Starr, J.L.; Jo, Y.-K. Nematicidal Effects of Silver Nanoparticles on Root-Knot Nematode in Bermudagrass. J. Nematol. **2014**, 46, 261–266.
56. Ardakani, A.S. Toxicity of Silver, Titanium and Silicon Nanoparticles on the Root-Knot Nematode, *Meloidogyne incognita*, and Growth Parameters of Tomato. Nematology **2013**, 15, 671–677, doi:https://doi.org/10.1163/15685411-00002710.
57. Rani, K.; Devi, N.; Banakar, P.; Kharb, P.; Kaushik, P. Nematicidal Potential of Green Silver Nanoparticles Synthesized Using Aqueous Root Extract of *Glycyrrhiza glabra*. Nanomaterials **2022**, 12, 2966, doi:10.3390/nano12172966.
58. Ghareeb, R.Y.; Shams El-Din, N.G.E.-D.; Maghraby, D.M.E.; Ibrahim, D.S.S.; Abdel-Megeed, A.; Abdelsalam, N.R. Nematicidal Activity of Seaweed-Synthesized Silver Nanoparticles and Extracts against *Meloidogyne incognita* on Tomato Plants. Sci. Rep. **2022**, 12, 3841, doi:10.1038/s41598-022-06600-1.

59. Lallo Da Silva, B.; Abuçafy, M.P.; Berbel Manaia, E.; Oshiro Junior, J.A.; Chiari-Andréo, B.G.; Pietro, R.C.R.; Chiavacci, L.A. Relationship Between Structure and Antimicrobial Activity of Zinc Oxide Nanoparticles: An Overview. Int. J. Nanomedicine **2019**, Volume 14, 9395–9410, doi:10.2147/IJN.S216204.
60. Ndolomingo, M.J.; Bingwa, N.; Meijboom, R. Review of Supported Metal Nanoparticles: Synthesis Methodologies, Advantages and Application as Catalysts. J. Mater. Sci. **2020**, 55, 6195–6241, doi:10.1007/s10853-020-04415-x.
61. Javed, Z.; Dashora, K.; Mishra, M.; D. Fasake, V.; Srivastva, A. Effect of Accumulation of Nanoparticles in Soil Health- a Concern on Future. Front. Nanosci. Nanotechnol. **2019**, 5, doi:10.15761/FNN.1000181.
62. Ajiboye, T.T.; Ajiboye, T.O.; Babalola, O.O. Impacts of Binary Oxide Nanoparticles on the Soybean Plant and Its Rhizosphere, Associated Phytohormones, and Enzymes. Molecules **2023**, 28, 1326, doi:10.3390/molecules28031326.
63. Ballikaya, P.; Mateos, J.M.; Brunner, I.; Kaech, A.; Cherubini, P. Detection of Silver Nanoparticles inside Leaf of European Beech (*Fagus sylvatica* L.). Front. Environ. Sci. **2023**, 10, 1107005, doi:10.3389/fenvs.2022.1107005.
64. Abdellatif, K.F.; Abdelfattah, R.H.; El-Ansary, M.S.M. Green Nanoparticles Engineering on Root-Knot Nematode Infecting Eggplants and Their Effect on Plant DNA Modification. Iran. J. Biotechnol. **2016**, 14, 250–259, doi:10.15171/ijb.1309.
65. Nazir, K.; Mukhtar, T.; Javed, H. In Vitro Effectiveness of Silver Nanoparticles against Root-Knot Nematode (*Meloidogyne incognita*). Pak. J. Zool. **2019**, 51, doi:10.17582/journal.pjz/2019.51.6.2077.2083.
66. Rossbach, L.M.; Oughton, D.H.; Maremonti, E.; Coutris, C.; Brede, D.A. In Vivo Assessment of Silver Nanoparticle Induced Reactive Oxygen Species Reveals Tissue Specific Effects on Cellular Redox Status in the Nematode *Caenorhabditis elegans*. Sci. Total Environ. **2020**, 721, 137665, doi:10.1016/j.scitotenv.2020.137665.
67. Tuncsoy, B. *Nematicidal Activity of Silver Nanomaterials against Plant-Parasitic Nematodes*. In Silver Nanomaterials for Agri-Food Applications; Elsevier, 2021; pp. 527–548 ISBN 978-0-12-823528-7.
68. Dzięgielewska, M.; Skwiercz, A.; Wesołowska, A.; Kozacki, D.; Przewodowski, W.; Kulpa, D. Effects of Silver, Gold, and Platinum Nanoparticles on Selected Nematode Trophic Groups; PREPRINT (Version 1) available at Research Square https://doi.org/10.21203/rs.3.rs-2973378/v1.
69. Brasil, Ministério da Saúde. Secretaria de Vigilância em Saúde. *Vigilância e controle da qualidade da água para consumo humano*; Ms: Brasília: Ministério da Saúde, 2006; 212 p. ISBN 978-85-334-1240-8.